Wood Sci Technol (2005)
DOI 10.1007/s00226-005-0021-1

ORIGINAL

P. D. Jones · L. R. Schimleck · G. F. Peter
R. F. Daniels · A. Clark III

Non-destructive estimation of *Pinus taeda* L tracheid morphological characteristics for samples from a wide range of sites in Georgia

Received: 18 January 2005

Abstract Tracheid coarseness, specific surface, wall thickness, perimeter, and radial and tangential diameter from 119 radial strips of *Pinus taeda* L. (loblolly pine) trees grown on 14 sites in three physiographic regions of Georgia (USA) were measured by SilviScan. NIR spectra were also collected in 10 mm increments from the radial longitudinal surface of each strip and split into calibration (9 sites, 729 spectra) and prediction sets (6 sites, 225 spectra). NIR spectra (untreated and mathematically treated first and second derivative and multiplicative scatter correction) were correlated with tracheid properties to develop calibrations for the estimation of these properties. Strong correlations were obtained for properties related to density, the strongest R^2 being 0.80 (coarseness), 0.78 (specific surface) and 0.84 (wall thickness). When applied to the test set, good relationships were obtained for the density-related properties (R_p^2 ranged from 0.68 to 0.86), but the accuracy of predictions varied depending on math treatment. The addition of a small number of cores fro'm the prediction set (one core per new site) to the calibration set improved the accuracy of predictions and, importantly, minimized the differences obtained with the various math treatments. These results suggest that density related properties can be estimated by NIR with sufficient accuracy to be used in operational settings.

P. D. Jones (✉) · L. R. Schimleck · R. F. Daniels
Warnell School of Forest Resources, The University of Georgia,
Athens, GA30602-2152, USA
E-mail: pdj7477@owl.forestry.uga.edu

G. F. Peter
School of Forest Resources and Conservation, University of Florida,
Gainesville, FL32611, USA

A. Clark III
USDA Forest Service, Southern Research Station, Athens, GA30602, USA

Introduction

In the Southeastern USA, *Pinus taeda* L. (loblolly pine) is the dominant plantation species owing to its ability to grow on a wide range of sites and the suitability of its wood for the manufacture of a wide range of forest products. Research directed at genetic improvement and the refinement of silvicultural practices has provided substantial improvements in the growth and yield of *P. taeda* (Li et al. 1999). The inclusion of quality traits such as stem straightness and wood quality in *P. taeda* breeding programs would greatly increase genetic gains and also the value of the trees (Li et al. 1999). Unfortunately, traditional methods for measuring wood properties are slow and cost prohibitive, limiting their inclusion in tree-breeding programs. Thus, lower cost and more rapid methods for measuring wood properties are required.

Near infrared (NIR) spectroscopy has the potential to provide the forest industry with a low cost and rapid tool for the non-destructive estimation of the chemical (Birkett and Gambino 1988; Garbutt et al. 1992; Michell 1995; Raymond and Schimleck 2002; Schimleck et al. 2000; Wright et al. 1990) and physical–mechanical properties of wood (Gindl et al. 2001; Hoffmeyer and Pedersen 1995; Meder et al. 2003; Schimleck et al. 1999; Thumm and Meder 2001; Thygesen 1994). It has also been demonstrated that fundamental tracheid morphological characteristics such as wall thickness (Schimleck and Evans 2004) and length (Hauksson et al. 2001; Schimleck et al. 2004) can be determined by NIR spectroscopy. Such properties are important in determining pulp fiber quality and paper performance, but their consideration in tree-breeding programs has been limited owing to the difficulties of routine measurement.

The study of Schimleck and Evans (2004) with *Pinus radiata* D. Don utilized data provided by the SilviScan instruments to develop calibrations for tracheid coarseness, perimeter, radial diameter, tangential diameter and wall thickness but were based on a relatively small sample set (8 cores, 119 spectra). Coefficients of determination (R^2) ranged from 0.65 for tracheid radial diameter to 0.91 for coarseness. The calibrations, apart from tracheid perimeter and tracheid radial diameter, performed well when applied to a separate test set of two cores that were from the same population as the calibration samples. However, it is unknown if strong calibrations for these morphological traits can be obtained using wood cores from a larger and more diverse set of *P. taeda* trees.

If NIR spectroscopy is to be used in tree breeding or in other forestry operations, robust calibrations based on large sample sets that encompass most of the variation in genotypes and environments (sites and physiographic regions) will need to be developed. Recently, Jones et al. (2005) developed robust calibrations for air-dry density, microfibril angle and stiffness using a large set of *P. taeda* wood cores obtained from nine different sites representing three different physiographic regions (Upper and Lower Coastal Plain, and Piedmont) in Georgia (USA). The calibrations reported by Jones et al. (2005) had R^2 that ranged from 0.78 (air-dry density) to 0.93 (stiffness) and while having larger calibration errors than those reported by Schimleck and Evans (2002a, 2002b, 2003), demonstrated that calibrations for these properties could be obtained using a highly diverse population of trees. Hence, it may also be

possible to obtain good calibrations for tracheid morphological characteristics using large, diverse set of samples. The objectives of this study were:

1. to create calibrations for tracheid morphological characteristics (coarseness, perimeter, radial diameter, specific surface, tangential diameter and wall thickness) using samples drawn from a wide variety of sites chosen to represent the three physiographic regions where *P. taeda* is grown in Georgia, USA;
2. to examine the performance of the tracheid morphology calibrations when applied to samples from sites not included in the calibration; and
3. to improve the applicability of tracheid morphological trait calibrations to samples from sites not initially included in the calibration set.

Materials and methods

Sample origin

Samples were collected from *P. taeda* plantations located in Georgia, USA. For each of the three physiographic regions in Georgia where *P. taeda* is grown (Lower and Upper Atlantic Costal Plain, and Piedmont), five plantations, ranging in age from 21 to 26 years, with different site indices were sampled. The characteristics of the sites are summarized in Table 1. The calibration set was comprised of 90 breast height (1.37 m) increment cores sampled from three plantations within each region; ten increment cores per site were taken. One increment core developed blue stain and was unavailable for analysis because of discoloration, leaving 89 cores for analysis. The prediction set was comprised of 30 breast height increment cores (five cores per plantation, two plantations per region).

Table 1 Stand descriptions for samples used in the calibration and prediction sets including age, site index (SI_{25}), county, latitude (Lat.), longitude (Long.) and physiographic region

Region	SI_{25}	Age	County	Lat.	Long.
Calibration set					
Upper Atlantic Coastal Plain	67	24	Marion	32°33′	−84°60′
Upper Atlantic Coastal Plain	69	25	Wilkinson	32°78′	−82°97′
Upper Atlantic Coastal Plain	78	22	Clay	31°62′	−84°99′
Lower Atlantic Coastal Plain	76	25	Effingham	32°26′	−81°27′
Lower Atlantic Coastal Plain	79	25	Glynn	31°31′	−81°60′
Lower Atlantic Coastal Plain	84	25	Camden	31°11′	−81°81′
Piedmont	54	25	Greene	33°70′	−83°22′
Piedmont	55	21	Polk	34°09′	−85°22′
Piedmont	61	26	Jones	32°96′	−83°62′
Prediction set					
Upper Atlantic Coastal Plain	55	22	Stewart	32°13′	−84°70′
Upper Atlantic Coastal Plain	67	24	Marion	32°34′	−84°60′
Lower Atlantic Coastal Plain	80	25	Wayne	31°42′	−81°68′
Lower Atlantic Coastal Plain	81	24	Liberty	31°79′	−81°57′
Piedmont	54	24	Talbot	32°77′	−84°61′
Piedmont	66	26	Greene	33°46′	−83°10′

SilviScan analysis

One hundred and nineteen radial wooden strips were available for SilviScan analysis; these strips were cut from increment cores using a twin-blade saw. Strip dimensions were 2 mm tangentially, and 7 mm longitudinally; radial length was determined by the pith-to-bark length of the sample. The radial strips were extracted in 30°C acetone for 24 h prior to SilviScan analysis.

The SilviScan-1 image analysis system (Evans 1994) was used to determine radial tracheid dimensions (R) and tangential tracheid dimensions (T). Tracheid coarseness (C), perimeter (external perimeter of rectangular tracheid cross-section, P), specific surface (S), and tracheid wall thickness (w) were determined from relationships that have been in use in various forms for several decades (Evans 1994):

$$P = 2(R + T) \tag{1}$$

$$C = \mathrm{RTD} \tag{2}$$

$$w = P/8 - 1/2(P/16 - C/d)^{1/2} \tag{3}$$

$$S = P/C \tag{4}$$

D is air-dry density and was determined using X-ray densitometry on SilviScan-1 (Evans 1994) and d is approximately equal to 1,500 kg/m^3 for all softwoods (Kellogg et al. 1975).

All measurements were made in a conditioned atmosphere maintained at 40% RH and 20°C (giving sample moisture content of approximately 8%). The image analysis data provided by Silviscan-1 were obtained in 50 μm steps. Averages were then determined for all tracheid morphological characteristics over 10-mm sections from pith to bark for correlation with the NIR data.

NIR spectroscopy

Diffuse reflectance NIR spectra were collected from the radial face of each strip using a NIR Systems Inc. Model 5000 scanning spectrometer. Samples were held in a custom-made holder (Schimleck et al. 2001). A 5 mm×10 mm mask, which was used to ensure an area of constant size, was analyzed. The spectra were collected at 2-nm intervals over the wavelength range 1,100–2,500 nm. The instrument reference was a ceramic standard. Fifty scans were accumulated for each 10 mm section; these scans were averaged to give a single spectrum per section. All measurements were made in a controlled environment of 40% relative humidity and a temperature of 20°C. A total of 729 spectra were collected from the 89 radial strips representing the calibration set, and 225 spectra were collected from the 30 radial strips representing the prediction set. Table 2 shows the summary statistics for the two data sets.

Tracheid morphological characteristic calibrations

Calibrations for the tracheid morphological characteristics were developed using the Unscrambler (version 8.0) software package (Camo AS, Norway). Three math treatments; first and second derivatives (obtained from the

Table 2 Summary of variation in tracheid morphological traits of samples used for the calibration and prediction sets

Tracheid morphological characteristic	Calibration set (729 spectra)				Prediction set (225 spectra)			
	Minimum	Maximum	Av.	Std. dev.	Minimum	Maximum	Av.	Std. dev.
Density related correlated properties								
Coarseness (μg/m)	334.56	784.44	515.27	83.02	338.03	731.60	526.56	94.72
Specific surface (m^2 /kg)	180.81	379.46	264.45	35.21	191.71	353.81	261.64	37.76
Wall thickness (μm)	1.90	5.10	3.28	0.63	2.09	5.00	3.31	0.69
Image analysis derived								
Perimeter (μm)	107.98	142.86	125.38	5.86	108.18	146.64	126.66	6.17
Radial diameter (μm)	26.52	39.20	32.68	2.15	26.94	40.46	32.89	2.11
Tangential diameter (μm)	26.65	35.42	30.01	1.59	26.80	35.30	30.43	1.73

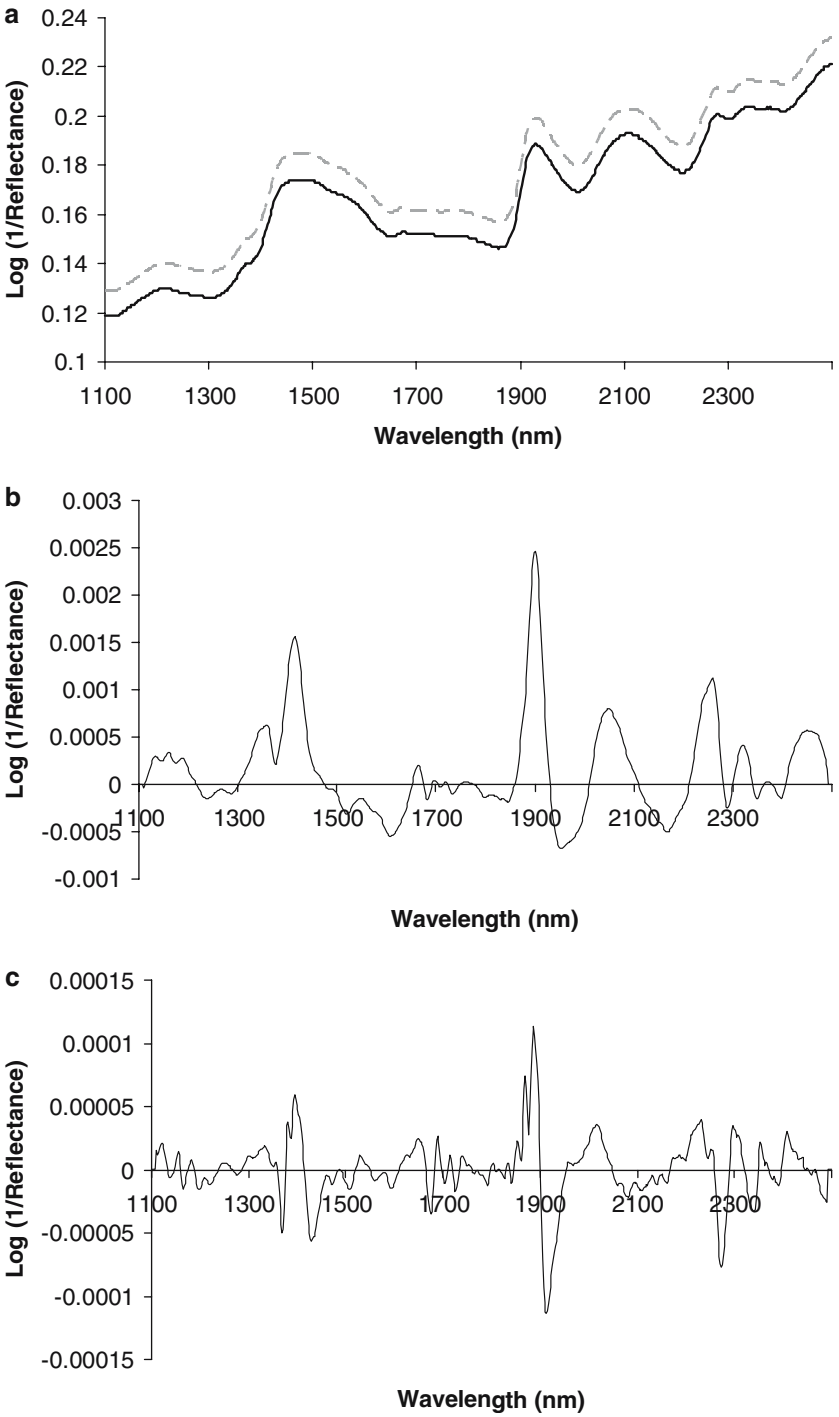

Fig. 1 Spectrum of an individual sample and the effect of each math treatment on the spectrum: raw (*solid black line*) and MSC (*dashed gray line*) (**a**), first derivative (**b**) and second derivative (**c**)

untreated spectra using the Savitzky–Golay approach, with left and right gaps of 8 nm) and multiplicative scatter correction (MSC) (Naes et al. 2002) along with the raw spectral data were used to create the calibrations using partial least squares (PLS) regression. Figure 1 shows the effect of the different math treatments on an individual spectrum: (a) raw (solid black line) and MSC transformation (dashed gray line), (b) shows the first derivative and (c) illustrates the second derivative. All three methods are known to reduce noise that occurs within spectral data (Naes et al. 2002). Calibrations were developed with four cross validation segments.

The standard error of calibration (SEC) (determined from the residuals of the final calibration), the standard error of cross validation (SECV) (determined from the residuals of each cross validation phase), the coefficient of determination (R^2), and the ratio of performance to deviation (RPD_c) (Williams and Sobering 1993), calculated as the ratio of the standard deviation of the reference data to the SECV, were used to assess calibration performance. Determination of RPD allows the comparison of calibrations developed for different wood properties that have differing data ranges and units; the higher the RPD_c, the more accurate the data is described by the calibration.

Prediction of wood properties

To examine the performance of the calibrations, they were used to predict the tracheid morphological characteristics (coarseness, perimeter, radial diameter, specific surface, tangential diameter and wall thickness) of the test set samples. The standard error of prediction (SEP) (determined from the residuals of the predictions) was calculated, which gives a measure of how well a calibration predicts parameters of interest for set of samples not included in the calibration set. The predictive ability of the calibrations was assessed by calculating the RPD_p (which is similar to the RPD_c) but uses the standard deviation of the prediction set reference data and the SEP.

Results

The tracheid morphological characteristics examined in this study can be classified into two distinct groups. The first group includes properties strongly related to density (coarseness, specific surface and wall thickness), while the second group includes properties measured by image analysis (tracheid perimeter and radial and tangential diameter). Because of the interrelationships between the different morphological characteristics, we examined how each of the characteristics were related in a pair-wise manner (Table 3). Air-dry density has strong relationships with coarseness ($R^2 = 0.86$), specific surface (−0.93) and wall thickness (0.97) as expected. Similarly coarseness, specific surface and wall thickness are strongly correlated with each other. The relationships of coarseness and wall thickness with density were similar to those reported by Schimleck and Evans (2004) for *P. radiata*. The properties measured using image analysis also show strong relationships with each other, but not with any of the density-related properties.

Table 3 Coefficients of determination between SilviScan measured morphological traits

	Density (kg/m^3)	Coarseness (μg/m)	Specific surface (m^2 /kg)	Wall thickness (μm)	Perimeter (μm)	Radial diameter (μm)	Tangential diameter (μm)
Density (kg/m^3)	1						
Coarseness (μg/m)	0.86	1					
Specific surface (m^2 /kg)	−0.93	−0.92	1				
Wall thickness (μm)	0.97	0.95	−0.95	1			
Perimeter (μm)	−0.11	0.37	−0.06	0.10	1		
Radial diameter (μm)	0.01	0.01	0.25	−0.26	0.85	1	
Tangential diameter |(μm)	0.13	0.67	−0.44	0.53	0.70	0.98	1

Calibrations and predictions

Density-related properties

All of the density-related properties gave reasonable calibrations (Table 4). R^2 for the coarseness calibrations ranged from 0.76 (raw and MSC treated spectra) to 0.80 (second derivative-treated spectra), while calibration errors were similar

Table 4 Summary of calibrations and predictions obtained using untreated and math-treated NIR spectra collected in 10 mm sections from the radial longitudinal face of radial wooden strips for coarseness, specific surface, wall thickness, perimeter, radial diameter and tangential diameter. Calibration statistics include the coefficient of determination(R^2, R^2_p), the standard error of calibration (SEC), the standard error of cross validation (SECV), the standard error of prediction (SEP) and the ratio of performance to standard deviation (RPD_c and RPD_p)

Math treatment		Calibration					Prediction		
		Factors	R^2	SEC	SECV	RPD_c	R^2_p	SEP	RPD_p
Coarseness (μg/m)	Raw	7	0.76	40.70	41.47	2.00	0.71	116.56	0.81
	MSC	6	0.76	40.40	41.13	2.02	0.81	75.51	1.25
	1st Derivative	5	0.77	39.64	40.60	2.04	0.82	45.07	2.10
	2nd Derivative	6	0.80	37.55	40.97	2.03	0.83	65.80	1.44
Specific surface (m^2 /kg)	Raw	7	0.77	16.81	17.22	2.04	0.68	37.62	1.00
	MSC	5	0.76	17.28	17.59	2.00	0.77	35.35	1.07
	1st Derivative	5	0.78	16.60	17.11	2.06	0.78	26.48	1.43
	2nd Derivative	3	0.73	18.33	18.63	1.89	0.77	20.47	1.84
Wall thickness (μm)	Raw	7	0.84	0.25	0.26	2.44	0.81	0.78	0.88
	MSC	6	0.84	0.25	0.26	2.46	0.86	0.68	1.02
	1st Derivative	5	0.84	0.25	0.26	2.41	0.86	0.26	2.66
	2nd Derivative	3	0.80	0.28	0.29	2.20	0.80	0.32	2.15
Perimeter (μm)	Raw	10	0.42	4.47	4.56	1.29	0.37	7.36	0.84
	MSC	9	0.42	4.45	4.54	1.29	0.33	9.12	0.68
	1st Derivative	10	0.49	4.18	4.45	1.32	0.53	4.62	1.33
	2nd Derivative	7	0.50	4.14	4.64	1.26	0.41	8.31	0.74
Radial diameter (μm)	Raw	10	0.39	1.68	1.72	1.25	0.25	2.83	0.75
	MSC	10	0.39	1.68	1.73	1.25	0.28	3.66	0.58
	1st Derivative	10	0.46	1.58	1.70	1.27	0.42	1.77	1.20
	2nd Derivative	7	0.46	1.58	1.78	1.21	0.29	1.79	1.18
Tangential diameter (μm)	Raw	10	0.59	1.01	1.04	1.53	0.58	1.21	1.43
	MSC	10	0.62	0.98	1.01	1.57	0.58	1.22	1.41
	1st Derivative	6	0.60	1.00	1.01	1.56	0.63	1.09	1.59
	2nd Derivative	6	0.64	0.95	1.02	1.56	0.59	1.17	1.47

with RPD_c ranging from 2.00 (untreated spectra) to 2.04 (first derivative treated spectra). Specific surface calibrations yielded R^2 ranging from 0.73 (second derivative treated spectra) to 0.78 (first derivative-treated spectra) and also had similar levels of calibration error despite the number of factors used varying from 3 to 7. The calibrations for wall thickness gave the strongest R^2 (0.84 for Raw, MSC, and first derivative-treated spectra), and had RPD_c values ranging from 2.20 (second derivative-treated spectra) to 2.46 (MSC treated spectra). Figure 2 illustrates the calibrations for coarseness (a) and wall thickness (b) using MSC-treated spectra.

The principle test of a calibration is to use it in prediction of a set of samples unrelated to those used to develop the calibration. Table 4 summarizes the results for predictions made on the separate test set (225 spectra collected from 30 cores representing six sites not included in the calibration). A prediction $R^2(R_p^2)$ was calculated as the proportion of variation in the independent prediction set that was explained by the calibration. In general, the wood property calibrations developed using different math treated spectra gave similar R_p^2 but the SEP and consequently the RPD_p varied greatly between math treatments (Table 4).

Regardless of math treatment, the coarseness calibrations provided reasonable R_p^2 ranging from 0.71 to 0.83; however, the RPD_p varied from 0.81 (untreated spectral data) to 2.10 (first derivative-treated data). Figure 3 compares predictions of coarseness obtained using the untreated spectra (a) and the first derivative-treated spectra (b). Figure 2 highlights the effect that the different math treatments have on the predictive accuracy of the coarseness calibrations. Predictions of coarseness based on the untreated spectra (a) have a large amount of error because they deviate from the line of equivalence (light gray dashed line); while predictions of coarseness based on the first derivative-treated spectra (b) lie almost upon the line.

Predictions of specific surface using the first derivative-treated spectra gave the highest R_p^2 (0.78), while predictions based on the untreated spectra had the lowest R_p^2 (0.68) (Table 4). Of the three density-related properties, wall thickness predictions gave the highest R_p^2 (0.86, obtained using MSC and first derivative-treated spectra). However, RPD_p for the two math treatments were quite different, 1.02 (MSC-treated spectra) and 2.66 (first-derivative treated spectra) (Table 4).

Image analysis-derived properties

The image analysis-derived properties did not provide calibration statistics as strong as those obtained for the density-related properties (Table 4). The strongest R^2 obtained for the perimeter and radial diameter calibrations were 0.50 (second-derivative treated spectra) and 0.46 (first- and second-derivative treated spectra), respectively. Calibrations for tangential diameter faired better with R^2 ranging from 0.59 (untreated spectra) to 0.64 (second-derivative treated spectra), while the best RPD_c was 1.57 for the MSC-treated spectra.

When the calibrations were applied to the test set, the calibrations for tangential diameter provided the strongest predictions with R_p^2 ranging from 0.58 (MSC-treated spectra) to 0.63 (first derivative-treated spectra), while RPD_p values for the same math treatments ranged from 1.41 to 1.59. Predictions of

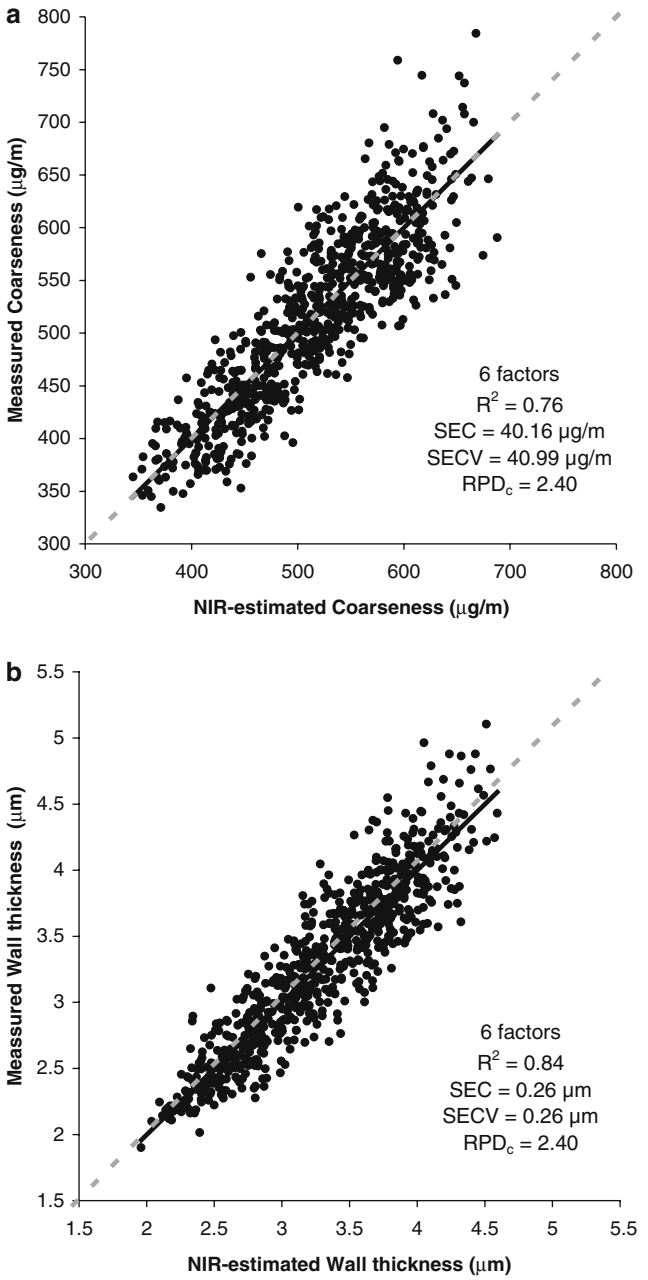

Fig. 2 Relationship between SilviScan measured coarseness and NIR-estimated coarseness (**a**) and measured wall thickness and NIR-estimated wall thickness (**b**). MSC-treated spectra were used for both calibrations. The *dashed gray line* represents the line of equivalence

perimeter and radial diameter were poor with the highest R^2_p being 0.53 for perimeter (first derivative-treated spectra) and 0.42 for radial diameter (first derivative-treated spectra).

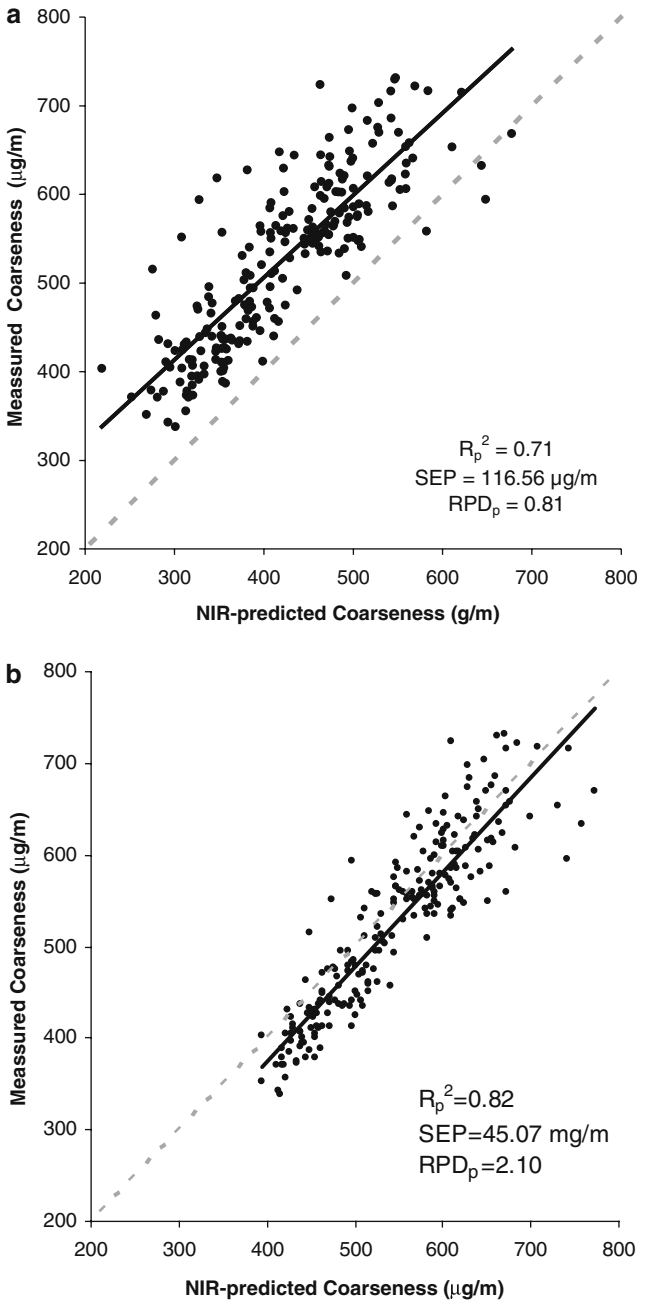

Fig. 3 Prediction results for coarseness using two different math treatments, untreated spectra (**a**) and first-derivative treated spectra (**b**). The *dashed gray line* represents the line of equivalence

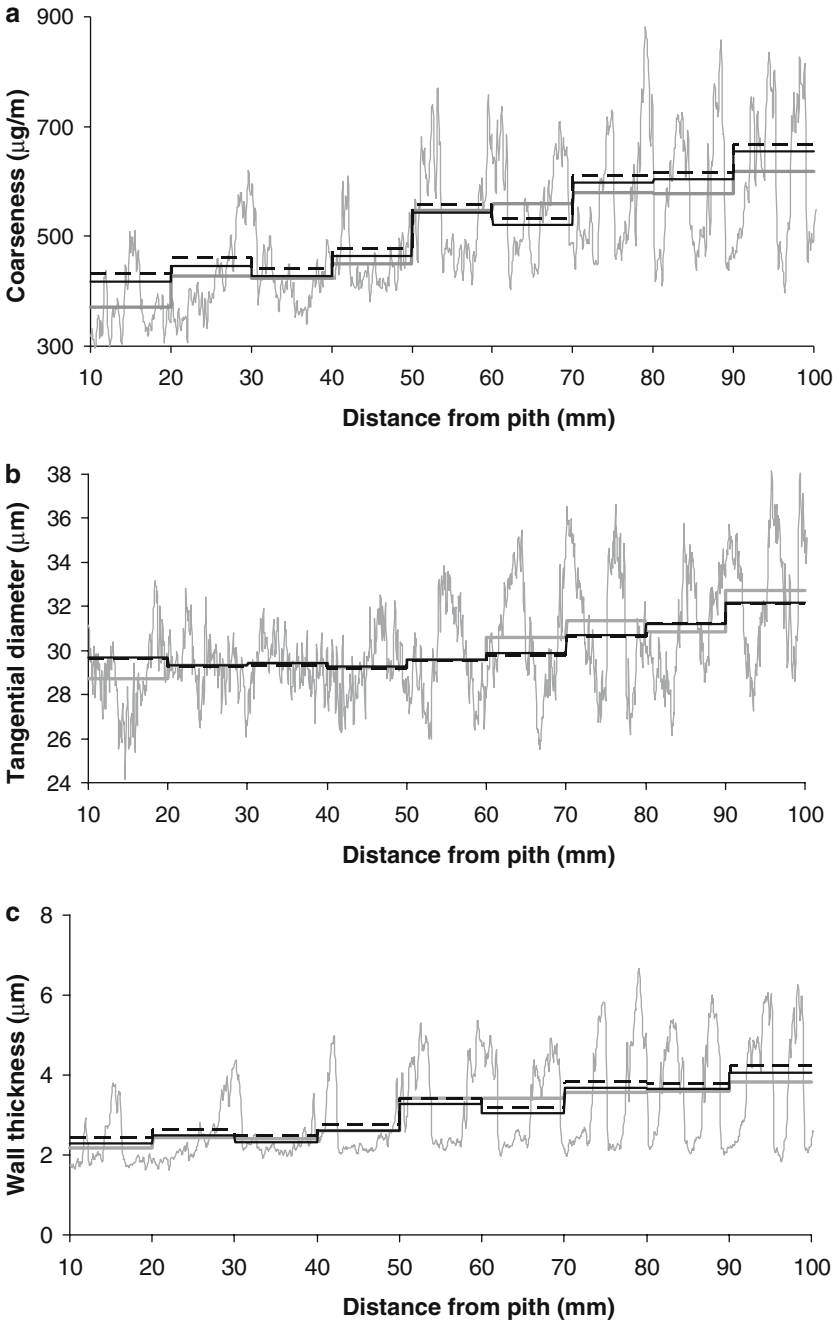

Fig. 4 Plot of pith-to-bark radial variation for (**a**) coarseness, (**b**) tangential diameter and (**c**) wall thickness for a randomly selected *P. taeda* radial strip. The *solid thin gray line* represents the original SilviScan data, the *solid thick gray line* represents SilviScan data averaged over 10 mm, the *dashed black line* represents values predicted by the original calibrations and the *solid black line* represents values predicted using the expanded calibrations

Table 5 Summary of the most important wavelength for each morphological property and respective math treatment

Property	Math treatment			
	Raw (nm)	MSC (nm)	1st Derivative (nm)	2nd Derivative (nm)
Coarseness	2,086	2,498	1,412	1,876
Specific surface	2,086	2,498	1,412	1,876
Wall thickness	2,086	2,498	1,412	1,876
Perimeter	1,102	1,974	1,902	1,868
Radial diameter	2,126	2,496	1,412	1,876
Tangential diameter	1,492	2,498	1,906	1,492

Table 5 shows the most important wavelength for each morphological property and respective math treatment. For each of the density-related properties, the most important wavelength was the same. Calibrations for image analysis-derived properties used different wavelengths.

Table 6 Summary of enhanced calibrations and predictions obtained using untreated and math-treated NIR spectra collected in 10 mm sections from the radial longitudinal face of radial wooden strips for coarseness, specific surface, wall thickness, perimeter, radial diameter and tangential diameter. Calibration statistics include the coefficient of determination (R^2 and R^2_p), the standard error of calibration (SEC), the standard error of cross validation (SECV), the standard error of prediction (SEP) and the ratio of performance to standard deviation (RPD_c and RPD_p)

Math treatment		Calibration					Prediction		
		Factors	R^2	SEC	SECV	RPD_c	R^2_p	SEP	RPD_p
Coarseness (μg/m)	Raw	8	0.76	40.66	41.50	2.02	0.78	44.99	2.11
	MSC	7	0.77	40.16	40.99	2.04	0.58	40.80	2.32
	1st Derivative	5	0.77	40.08	41.14	2.03	0.83	46.65	2.03
	2nd Derivative	6	0.80	37.84	41.31	2.02	0.84	38.48	2.46
Specific surface (m^2 /kg)	Raw	8	0.77	17.00	17.52	2.02	0.79	18.21	2.07
	MSC	6	0.77	17.04	17.50	2.02	0.80	16.91	2.23
	1st Derivative	5	0.77	16.77	17.36	2.03	0.78	17.88	2.11
	2nd Derivative	3	0.73	18.31	18.68	1.89	0.79	17.57	2.15
Wall thickness (μm)	Raw	8	0.84	0.25	0.26	2.45	0.86	0.27	2.59
	MSC	6	0.83	0.26	0.26	2.40	0.86	0.25	2.74
	1st Derivative	5	0.84	0.26	0.26	2.40	0.87	0.27	2.57
	2nd Derivative	3	0.80	0.28	0.29	2.19	0.80	0.31	2.24
Perimeter (μm)	Raw	10	0.40	4.56	4.66	1.27	0.36	5.24	1.17
	MSC	8	0.40	4.56	4.64	1.27	0.33	5.39	1.14
	1st Derivative	10	0.48	4.25	4.51	1.31	0.53	4.49	1.37
	2nd Derivative	6	0.46	4.35	4.72	1.25	0.45	5.60	1.10
Radial diameter (μm)	Raw	10	0.38	1.69	1.73	1.24	0.33	1.86	1.14
	MSC	8	0.35	1.73	1.76	1.22	0.27	1.98	1.07
	1st Derivative	10	0.45	1.59	1.71	1.26	0.46	1.60	1.32
	2nd Derivative	4	0.33	1.76	1.83	1.17	0.24	2.35	0.90
Tangential diameter (μm)	Raw	10	0.59	1.04	1.06	1.52	0.58	1.18	1.46
	MSC	10	0.62	1.00	1.04	1.56	0.58	1.11	1.56
	1st Derivative	6	0.60	1.02	1.04	1.55	0.62	1.04	1.65
	2nd Derivative	6	0.63	0.98	1.04	1.55	0.36	1.03	1.68

Improvement of tracheid morphological characteristic calibrations and predictions

The predictive performance of calibrations can be improved by including a small number of samples from the prediction set in the calibration set (Guthrie and Walsh 2002; Jones et al. 2005). Table 6 summarizes the results for these enhanced wood property calibrations and predictions obtained after NIR spectra from a single randomly selected core from each of the sites in the prediction set was added to the calibration set. The new cores increased the number of spectra in the calibration set to 771 (95 increment cores). In general, the enhanced calibrations had statistics similar to those reported for the original calibrations (Table 4). However, prediction error was decreased and RPD_ps were improved for all but three of the enhanced calibrations.

Predictions of coarseness with the enhanced calibrations all had R^2_p greater than 0.78 and RPD_ps greater than 2.0. With the exception of the coarseness calibration based on first-derivative treated spectra, the other enhanced coarseness calibrations all provided considerable reductions in predictive errors. The coarseness calibration based on untreated spectra demonstrated the largest improvement with RPD_p increasing from 0.81 to 2.11. For specific surface, the enhanced calibrations all provided decreases in prediction error. The largest improvement was for the MSC-treated data with a 108% increase in RPD_p. Predictions of wall thickness generally improved when the enhanced calibrations were used, the exception being results for the first derivative-treated spectra where the RPD_p fell from 2.66 to 2.57.

The image analysis-derived properties did not show the large reduction in prediction errors observed for coarseness, specific surface and wall thickness. Tangential diameter continued to have the highest R^2_p and RPD_p values, followed by perimeter and radial diameter.

In Fig. 4, radial variation for coarseness (a), tangential diameter (b) and wall thickness (c) are shown for a single, randomly selected sample from the prediction set. The figure includes SilviScan data at the original resolution, the SilviScan data averaged at 10 mm, predicted data at 10 mm using the original calibrations (based on first derivative treated spectra), and predicted data at 10 mm using the expanded calibrations again based on first-derivative treated spectra. Figure 4a–c shows that the data predicted by the respective calibrations corresponds closely to the SilviScan measured data, particularly for the enhanced calibrations.

Discussion

Three aspects important for the use of NIR spectroscopy for prediction of tracheid morphological characteristics have been examined. First, the use of a large sample size to create robust calibrations; second, the use of the calibrations to predict the properties of cores from sites not included in the calibration; and third, the enhancement of calibrations to reduce predictive error.

Development of calibrations using a large number of samples that contain a wide range of variation in the traits will give the best representation of the species as a whole. Berzaghi et al. (2002) successfully created calibrations for the chemical analysis of forage crops using a large sample size, showing that

with recent technological advancements large sample sets were manageable for creating calibrations. In the current study, 729 spectral samples were used to create calibrations, and to predict the variation of *P. taeda* tracheid morphological characteristics in plantations. Working with such large sample sets presents a number of practical difficulties. The handling and matching of spectral data and SilviScan data takes a great deal of patience and vigilance to assure that the proper data is matched with the scanned area. This can only be achieved through stringent data handling protocols. With an increase in resolution (i.e., spectra collected at 5 mm), the data sets will become larger and more complicated, but will allow for a greater understanding of wood properties, growth and age-dependent transitions in these properties, and possibly within ring estimation of wood properties using NIR spectroscopy. With previous work, calibrations had been performed using WinISI II (Infrasoft International 2000), as the data sets became larger ($n > 500$) the importation of constituents and the management of data became difficult because of the user interface; with Unscrambler, the importation of data is very intuitive because of its similarity to commonly used spreadsheet interfaces.

Calibrations for properties that are highly correlated with density gave promising results when applied to samples from sites other than those included in the calibrations. Wall thickness and coarseness are of particular importance for the pulp and paper industry as they help determine bonding potential of tracheids and individual fiber or tracheid strength (McKenzie 1994). Schimleck and Evans (2004) suggested that coarseness and wall thickness calibrations might decrease in accuracy using large data sets; this study demonstrates that with large data sets obtained from trees grown on a wide range of sites, strong calibrations can be developed for coarseness, specific surface and wall thickness. Schimleck and Evans (2004) examined the use of NIR to predict coarseness, wall thickness, perimeter, radial diameter and tangential diameter for *P. radiata* for a limited sample set (8 radial strips and 119 spectra). Calibrations based on second-derivative spectra gave SEC values of 31.0 μg/m and 0.2 μm for coarseness and wall thickness, respectively. When these calibrations were used to predict the properties of two different cores, from the same site, the resulting RPD_ps of the individual cores were 1.9 and 1.6 for coarseness and 2.7 and 1.4 for wall thickness (Schimleck and Evans 2004). This work demonstrated that NIR spectroscopy could predict some wood properties of *P. radiata*; however, their sample size was probably too small to develop calibrations robust enough to predict properties of samples from new populations (or sites). Here, we report that calibrations developed with a much larger and more diverse set of *P. taeda* wood cores resulted in SEC values of 37.55 μg/m for coarseness (non-enhanced calibration) and 0.28 μm for wall thickness (non-enhanced calibration) using the second-derivative data. The RPD_p values for the same two properties were 1.44 (coarseness) and 2.20 (wall thickness).

In this study the properties measured by image analysis did not produce calibrations adequate for predicting these properties, with the exception of tangential diameter. In contrast, Schimleck and Evans (2004) were able to obtain reasonable calibrations for radial and tangential diameter as well as perimeter. Radial diameter and tangential diameter were strongly related to each other (Table 3). Hence, similar calibration statistics could be expected for both properties, but this was not observed. It is possible that a stronger calibration was obtained for tangential diameter because of the orientation of the

NIR beam to the sample. Owing to our sampling methodology, NIR energy may have had a greater interaction with the tangential walls, and consequently, information relating to tangential diameter may be reflected in the spectra to a greater extent than that of radial diameter. The tangential diameter calibrations would only be useful for classification purposes or approximate estimations.

The predictive accuracy of the coarseness, specific surface and wall thickness calibrations can be enhanced by adding a single sample from new sites and by creating a new calibration. While not all expanded calibrations produced lower prediction errors, the expansion decreased the variability between prediction errors for the same properties using the differing math treatments.

Conclusions

This study demonstrates that large data sets that include a wide range of environmental and genetic variation can establish good calibrations for density-related tracheid morphological characteristics based on NIR spectra obtained in 10 mm sections from the radial face of *P. taeda* strips. Reasonable calibrations were obtained for tangential diameter, while the calibrations for perimeter and radial diameter were poor.

Calibrations for density-related properties gave strong relationships when used for predicting the tracheid morphologies of a separate set of cores from sites not included in the calibration set, but the accuracy of predictions varied depending on the math treatment employed. Predictions of tangential diameter had moderate relationships, while predictions of perimeter and radial diameter were poor.

The addition of a small number of cores from the prediction set (one core per site) to the calibration set minimized the difference between mathematical treatments and improved the accuracy of predictions for density related properties.

Acknowledgements The authors thank the UGA Wood Quality Consortium for *P. taeda* sample collection and the Georgia TIP^3 program for funding the SilviScan analysis of the samples. The authors would also like to thank the UGA Wood Quality Consortium for sample preparation and the SilviScan team for the determination of wood properties. Florida Agricultural Experiment Station Journal Series R-11045.

References

Birkett MD, Gambino MJT (1988) Potential applications for near-infrared spectroscopy in the pulping industry. Pap S Afr November/December:34–38

Evans R (1994) Rapid measurement of the transverse dimensions of tracheids in radial wood sections from *Pinus radiata*. Holzforschung 48:168–172

Garbutt DCF, Donkin MJ, Meyer JH (1992) Near-infrared reflectance analysis of cellulose and lignin in wood. Pap S Afr April:45–48

Gindl W, Teischinger A, Schwanninger M, Hinterstoisser B (2001) The relationship between near infrared spectra of radial wood surfaces and wood mechanical properties. J Near Infrared Spectrosc 9:255–261

Guthrie JA, Walsh KB (2002) Assessing and enhancing near infrared calibration robustness for soluble solids content in mandarin fruit. In: Near infrared spectroscopy. Proceedings of the 10th International Conference. NIR Publications, pp 151–154

Hauksson JB, Sjöstrom M, Edlund U, Bergqvist G, Bergsten U (2001) Prediction of basic wood properties for Norway spruce. Interpretation of near infrared spectroscopy data using partial least squares regression. Wood Sci Technol 35:475–485

Hoffmeyer P, Pedersen JG (1995) Evaluation of density and strength of Norway spruce wood by near-infrared reflectance spectroscopy. Holz Roh- Werkst 53:165–170
Jones PD, Schimleck LR, Peter GF, Daniels RF, Clark III A (2005) Nondestructive estimation of *Pinus taeda* L wood properties for samples from a wide range of sites in Georgia. Can J For Res 35:85–92
Kellogg RM, Wellwood RW, Sastry CBR (1975) Relationships between cell wall composition and cell wall density. Wood Fibre 7:170–177
Li B, McKeand S, Weir R (1999) Tree improvement and sustainable forestry—impact of two cycles of loblolly pine breeding in the USA. For Genet 6:229–234
McKenzie AW (1994) A guide to pulp evaluation. CSIRO, Australia
Meder R, Thumm A, Marston D (2003) Sawmill trial of at-line prediction of recovered lumber stiffness by NIR spectroscopy of *Pinus radiata* cants. J Near Infrared Spectrosc 11:137–143
Michell AJ (1995) Pulpwood quality estimation by near-infrared spectroscopic measurements on eucalypt woods. Appita J 48:425–428
Naes T, Isaksson T, Fearn T, Davies T (2002) A user-friendly guide to multivariate calibration and classification. NIR, Chichester
Raymond CA, Schimleck LR (2002) Development of near infrared reflectance analysis calibrations for estimating genetic parameters for cellulose content in *Eucalyptus globulus*. Can J For Res 32:170–176
Schimleck LR, Evans R (2002a) Estimation of microfibril angle of increment cores by near infrared spectroscopy. IAWA J 23:225–234
Schimleck LR, Evans R (2002b) Estimation of wood stiffness of increment cores by near infrared spectroscopy: the development and application of calibrations based on selected cores. IAWA J 23:217–224
Schimleck LR, Evans R (2003) Estimation of air-dry density of increment cores by near infrared spectroscopy. Appita J 56:312–317
Schimleck LR, Evans R (2004) Estimation of *Pinus radiata* D. Don tracheid morphological characteristics by near infrared spectroscopy. Holzforschung 58:66–73
Schimleck LR, Michell AJ, Raymond CA, Muneri A (1999) Estimation of basic density of *Eucalyptus globulus* using near-infrared spectroscopy. Can J For Res 29:194–201
Schimleck LR, Raymond CA, Beadle CL, Downes GM, Kube PD, French J (2000) Applications of NIR spectroscopy to forest research. Appita J 53:458–464
Schimleck LR, Evans R, Ilic J (2001) Estimation of *Eucalyptus delegatensis* wood properties by near infrared spectroscopy. Can J For Res 31:1671–1675
Schimleck LR, Jones PD, Peter GF, Daniels RF, Clark III A (2004) Nondestructive estimation of tracheid length from sections of radial wood strips by near infrared spectroscopy. Holzforschung 58:375–381
Thumm A, Meder R (2001) Stiffness prediction of radiata pine clearwood test pieces using near infrared spectroscopy. J Near Infrared Spectrosc 9:117–122
Thygesen LG (1994) Determination of dry matter content and basic density of Norway spruce by near-infrared reflectance and transmission spectroscopy. J Near Infrared Spectrosc 2:127–135
Williams PC, Sobering DC (1993) Comparison of commercial near infrared transmittance and reflectance instruments for the analysis of whole grains and seeds. J Near Infrared Spectrosc 1:25–33
Wright JA, Birkett MD, Gambino MJT (1990) Prediction of pulp yield and cellulose content from wood samples using near-infrared reflectance spectroscopy. Tappi J 73:164–166